

Enhanced Fluorescence Detection of Metal Ions Using Light-Harvesting Mesoporous Organosilica

Minoru Waki,^[a, b] Norihiro Mizoshita,^[a, b] Yoshifumi Maegawa,^[a, b] Takeru Hasegawa,^[b, c] Takao Tani,^[a, b] Toyoshi Shimada,^[b, c] and Shinji Inagaki^{*[a, b]}

Abstract: Enhanced fluorescence detection of metal ions was realized in a system consisting of a fluorescent 2,2'-bipyridine (BPy) receptor and light-harvesting periodic mesoporous organosilica (PMO). The fluorescent BPy receptor with two silyl groups was synthesized and covalently attached to the pore walls of biphenyl (Bp)-bridged PMO powder. The fluorescence intensity from the BPy receptor was significantly enhanced by the light-harvesting property of Bp-PMO, that is, the energy funneling into the BPy receptor

from a large number of Bp groups in the PMO framework which absorbed UV light effectively. The enhanced emission of the BPy receptor was quenched upon the addition of a low concentration of Cu²⁺ (0.15–1.2 × 10⁻⁶ M), resulting in the sensitive detection of Cu²⁺. Upon titration of Zn²⁺ (0.3–6.0 × 10⁻⁶ M), the fluorescence exci-

tation spectrum was systematically changed with an isosbestic point at 375 nm through 1:1 complexation of BPy and Zn²⁺ similar to that observed in BPy-based solutions, indicating almost complete preservation of the binding property of the BPy receptor despite covalent fixing on the solid surface. These results demonstrate that light-harvesting PMOs have great potential as supporting materials for enhanced fluorescence chemosensors.

Keywords: fluorescence • ligand effects • light harvesting • mesoporous materials • metal-ion detection

Introduction

Mesoporous silica is an ideal support material for sensitive receptors because of its high surface area (ca. 1000 m² g⁻¹) and uniform porosity.^[1–3] The high surface area allows doping with high concentrations of sensitive receptors, and the uniform porosity allows the facile diffusion of analytes (e.g., molecules and ions). The mechanical robustness and high processability of mesoporous materials are also great advantages in their practical applications. A variety of sensitive receptors have been anchored on the pore surfaces of mesoporous silicas through post-synthetic grafting or co-condensation for use in fluorescent chemosensors.^[1–3]

Periodic mesoporous organosilicas (PMOs), synthesized by surfactant-directed self-assembly of bridged organosilane precursors (R-[Si(OR')₃]_n; n ≥ 2, R = bridging organic group, R' = CH₃, C₂H₅, etc.), are unique hybrid materials in which functional organic groups (R) are densely and covalently embedded within the silica walls.^[4] There have been a large number of reports on the synthesis of PMOs containing various bridging organic groups in their frameworks,^[5] including highly luminescent organic fluorophores^[6] such as biphenyl,^[7] oligo(phenylenevinylene),^[8] and tetraphenylpyrene.^[9] Chandra et al. reported the application of a luminescent PMO bearing a diimine moiety to metal-ion detection.^[10]

The organization of two or more different fluorophores in nanometer-sized channel materials is important for the fabrication of highly functional donor–acceptor structures such as energy-transfer and energy-funneling systems.^[11] PMOs allow the fluorophores to be located in two spatially separated regions: in the pore walls and in the mesochannels.^[12] We recently reported unique light-harvesting antenna properties for PMOs doped with dye molecules in the mesochannels.^[13,14] The organic fluorophores in the pore walls absorbed light effectively and transferred their excitation energy to the dye molecules in the mesochannels through Förster resonance energy transfer (FRET). The efficient funneling of the excitation energy into the dye by FRET significantly enhanced the fluorescence emission from the dye. For example, biphenyl (Bp)-PMO doped with coumarin 1 dye showed a remarkable enhancement of the emission from the dye, in which light energy absorbed by a large number of Bp groups in the pore walls was transferred to a

[a] Dr. M. Waki, Dr. N. Mizoshita, Y. Maegawa, Dr. T. Tani, Dr. S. Inagaki
Toyota Central R&D Laboratories, Inc.
Nagakute, Aich 480-1192 (Japan)
Fax: (+81) 561-63-6507
E-mail: inagaki@mosk.tytlabs.co.jp

[b] Dr. M. Waki, Dr. N. Mizoshita, Y. Maegawa, T. Hasegawa, Dr. T. Tani, Dr. T. Shimada, Dr. S. Inagaki
Core Research for Evolutional Science and Technology (CREST)
Science and Technology Agency (JST)
Kawaguchi, Saitama 332-0012 (Japan)

[c] T. Hasegawa, Dr. T. Shimada
Department of Chemical Engineering
Nara National College of Technology
Yamatokoriyama, Nara 639-1080 (Japan)

Supporting information for this article is available on the WWW under <http://dx.doi.org/10.1002/chem.201102492>.

single dye molecule in the mesochannel with a large quantum efficiency.^[13] Light-harvesting PMOs have been successfully applied to an enhanced photocatalytic system of CO₂ reduction^[15] and to highly luminescent PMO films with tunable emission colors.^[9,16]

Here, we report the first application of a light-harvesting PMO to an enhanced metal-ion detection system. As illustrated in Figure 1, the emission from a fluorescent receptor

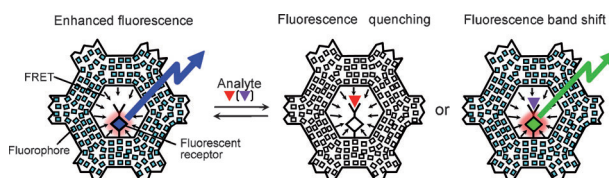
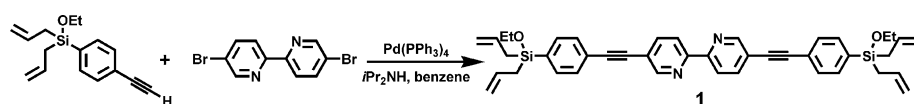


Figure 1. Schematic illustrations of enhanced fluorescence detection of analyte using a light-harvesting PMO.

attached in the mesochannels of PMO can be enhanced by the light-harvesting effect. The enhanced emission can be quenched or shifted in wavelength through the interaction between the receptor and an analyte, which results in sensitive analyte detection. Similar enhanced fluorescence detections based on FRET have been reported for zeolites,^[11] silica^[17] and polymer^[18] nanoparticles, micelles,^[19] self-assembled monolayers,^[20] Langmuir–Blodgett films,^[21] and dendrimers^[22] functionalized with fluorophores and receptors. Compared to these materials, PMOs have an ideal conformation of fluorophores and receptors, that is, numerous fluorophores surround a receptor placed in the rigid nanochannels, which offer great advantages such as a large enhancement effect and easy access of the analyte to the receptors. Amplified fluorescence chemosensors have also been reported for conjugated polymers, in which a single interaction with an analyte can quench a large number of fluorophores through exciton transport along the polymer chain.^[23] In this study, a novel BPy-bridged organosilane was synthesized and covalently attached on the pore walls of Bp-PMO powder. The BPy receptor in Bp-PMO was confirmed to show an enhancement of the fluorescence intensity by the light-harvesting effect, which successfully emphasized the change in emission intensity upon the addition of metal ions. In addition, the BPy receptor was found to show a similar binding property to that in BPy-based solution systems despite its covalent fixing on the solid surface.

Results and Discussion

Preparations of PMO with bipyridine receptor: The BPy moiety was selected as a receptor because it has typically been used as a strong ligand for transition metal ions, and has been incorporated in various molecular^[24] and polymer^[25] chemosensors for the detection of metal ions. A fluo-



Scheme 1. Preparation of fluorescent bipyridine receptor **1**.

rescent receptor containing the BPy ligand **1** was newly designed. The receptor **1** was synthesized by a coupling reaction of 5,5'-dibromo-2,2'-bipyridine with molecular building blocks of 1-diallylethoxysilyl-4-ethynylbenzene^[26] (Scheme 1). The attachment of phenylethynyl groups on both sides of the BPy expanded the π -conjugation length, which resulted in a red shift of the absorption band of the receptor from $\lambda_{\text{abs}} = 280$ to 350 nm. This red shift was favorable for efficient FRET from Bp-PMO to the receptor because the absorption band overlapped well with the emission band of Bp-PMO ($\lambda_{\text{em}} = 385$ nm) (Figure 2). A diallyle-

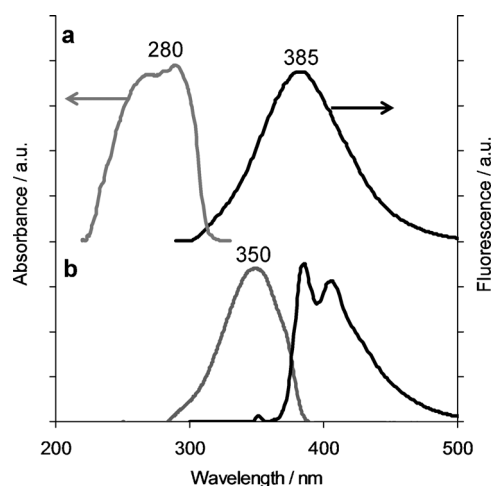
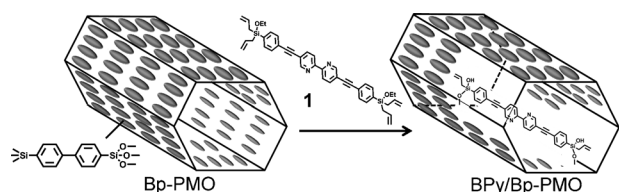


Figure 2. a) Fluorescence excitation (gray) and emission (black) spectra of Bp-PMO dispersed in CH₂Cl₂. b) Absorption (gray) and emission (black) spectra of BPy receptor **1** in CH₂Cl₂ (1.0×10^{-5} M).

thoxysilyl group was employed instead of a trialkoxysilyl group to bind the receptor to the surface silanol groups (Si-OH) in Bp-PMO. This substitution was made because the diallylethoxysilyl group is more stable than a trialkoxysilyl group during palladium-catalyzed coupling reactions and purification by silica gel chromatography,^[27] but it behaves as the synthetic equivalent of a trialkoxysilyl group, as reported by Shimada et al., who demonstrated the functionalization of silica surfaces using an allylorganosilane at the reflux temperature of toluene without any acid or base catalysts.^[28] In our preliminary experiments, the functionalization of Bp-PMO using receptor **1** with no catalyst was unsuccessful, possibly because of the lower acidity of the silanol groups in Bp-PMO than in silica.^[29] Therefore, we added a catalytic amount of trifluoroacetic acid to the starting suspension to promote the surface coupling reaction during reflux (Scheme 2). The amounts of BPy receptor loaded onto Bp-PMO, which were adjusted by the amount of **1** added to the



Scheme 2. Attachment of bipyridine receptor **1** onto the pore wall of Bp-PMO in refluxing toluene containing trifluoroacetic acid.

starting suspension, were finally determined to be 12, 27, 75, and 140 $\mu\text{mol g}^{-1}$ by a Total Nitrogen Analyzer, assuming that the detected nitrogen originated from the BPy receptor. The Bp-PMOs with attached BPy receptors are represented as BPy/Bp-PMO (X), where X is the BPy/Bp molar ratio of 0.003, 0.007, 0.020, or 0.038.

Figure 3a shows the X-ray diffraction (XRD) patterns of BPy/Bp-PMO with different BPy/Bp ratios. All the samples

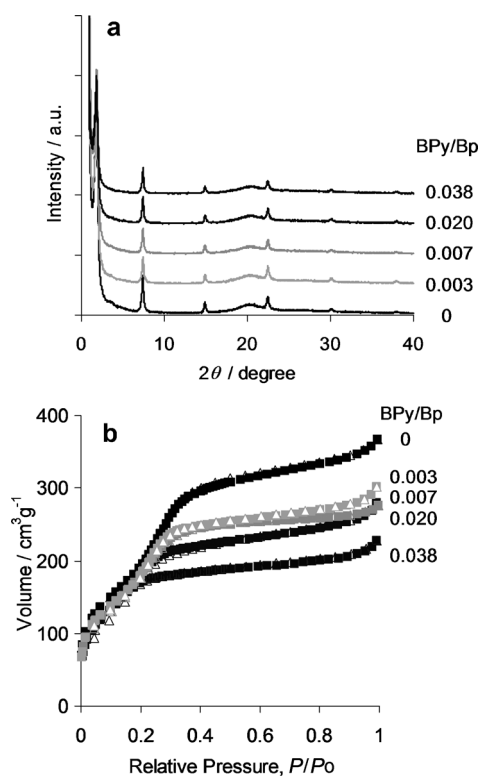


Figure 3. a) XRD patterns of BPy/Bp-PMO with different BPy/Bp ratios. b) Nitrogen adsorption isotherms of BPy/Bp-PMO with different BPy/Bp ratios.

showed clear diffraction patterns for both an ordered mesoporous structure ($2\theta = 1.82\text{--}1.86^\circ$, $d_{100} = 4.75\text{--}4.85$ nm) and a periodic arrangement of the Bp groups within the pore walls ($2\theta = 7.4, 14.9, 22.5, 30.1, \text{ and } 37.9^\circ$, $d = 1.19, 0.59, 0.40, 0.30, \text{ and } 0.24$ nm). The nitrogen adsorption/desorption isotherms were type IV, which is typical for an ordered mesoporous material, although the adsorption capacity gradually decreased with increasing BPy/Bp ratio (Figure 3b and

Table S1 in the Supporting Information). The average pore diameter also decreased, without a large decrease in the specific surface area. These results strongly suggest that **1** was successfully attached onto the pore surface of Bp-PMO. The ^{29}Si magic-angle spinning (MAS) NMR spectra of BPy/Bp-PMO (0.038) showed three signals at $-82.6, -73.0, \text{ and } -10.6$ ppm, corresponding to $\text{T}^3, \text{T}^2, \text{ and } \text{D}^1$ silicon species ($\text{T}^n: \text{RSi}(\text{OH})_{3-n}(\text{OSi})_n$, $n = 0\text{--}3$, $\text{D}^m: \text{R}_2\text{Si}(\text{OH})_{2-m}(\text{OSi})_m$, $m = 0\text{--}2$), respectively (Figure 4). The T^n silicon species were

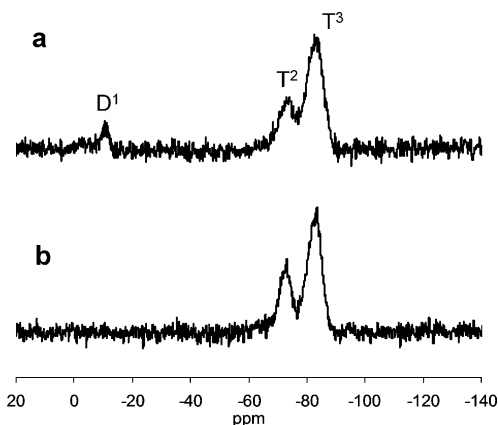


Figure 4. ^{29}Si MAS NMR of a) BPy/Bp-PMO and b) Bp-PMO.

attributed to the framework biphenyl-silica of Bp-PMO.^[7a] The D^1 silicon species was attributed to the silyl groups of the BPy receptor, which were condensed with silanol groups on the pore surface through elimination of the allyl groups (Scheme 2). There was no detection of uncondensed silicon species ($\text{S}^0: \text{R}_3\text{Si}(\text{OH}), \text{D}^0: (\text{R}_2\text{Si}(\text{OH})_2, \text{ and } \text{T}^0: (\text{RSi}(\text{OH})_3)$, suggesting that both sides of the silyl groups of the receptor **1** were attached on the surface. For the low BPy/Bp ratios (0.003, 0.007, and 0.020), the signals of the D^1 species were not clearly observed because the amounts of BPy receptor were too small to detect (Figure S1 in the Supporting Information). Figures 5a and 5b show the ^{13}C cross-polarization (CP)-MAS NMR spectra of BPy/Bp-PMO (0.038) and Bp-PMO, respectively. The signals of the BPy receptor overlapped with the original signals of Bp-PMO, so the differential spectrum was calculated between BPy/Bp-PMO and Bp-PMO (Figure 5c). This was very consistent with the ^{13}C NMR spectrum of the BPy receptor **1** in CDCl_3 (Figure 5d), indicating the successful anchoring of **1** in Bp-PMO.

Enhancement of fluorescence: Figures 6a and 6b show the fluorescence spectra of BPy/Bp-PMOs (0.003–0.038) excited at 350 and 280 nm, respectively. The 350 nm light was directly absorbed by the BPy receptor in Bp-PMO because the BPy receptor had much higher absorbance at this wavelength than Bp-PMO, as shown in Figure 2. However, the absorption efficiency of the light is not so high because of the low concentration of BPy receptors in Bp-PMO, which result in a relatively low-intensity fluorescence emission

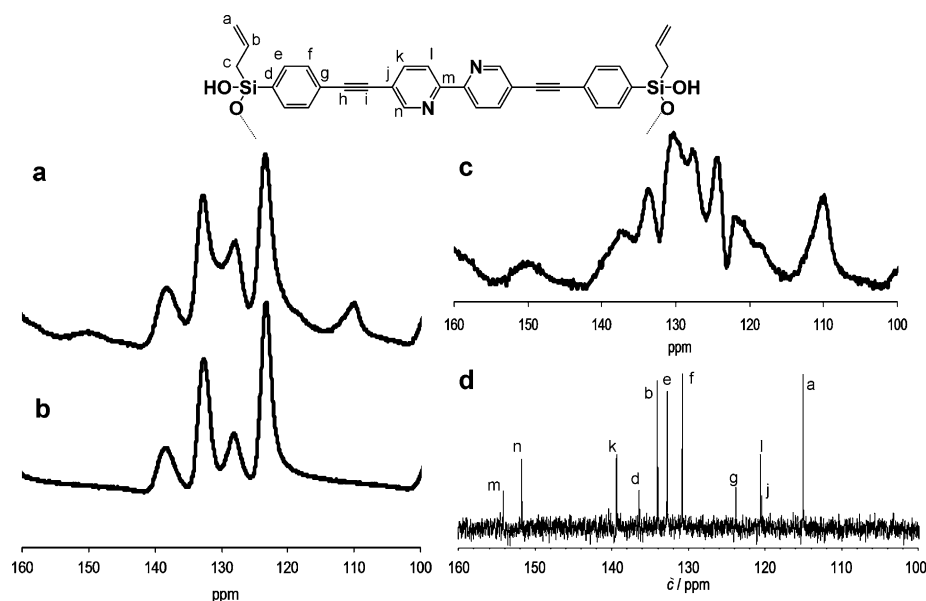


Figure 5. ^{13}C CP-MAS NMR spectra of a) BPy/Bp-PMO (0.038) and b) Bp-PMO. c) Differential spectrum between BPy/Bp-PMO (0.038) and Bp-PMO. d) ^{13}C NMR spectrum of BPy receptor **1** in CDCl_3 .

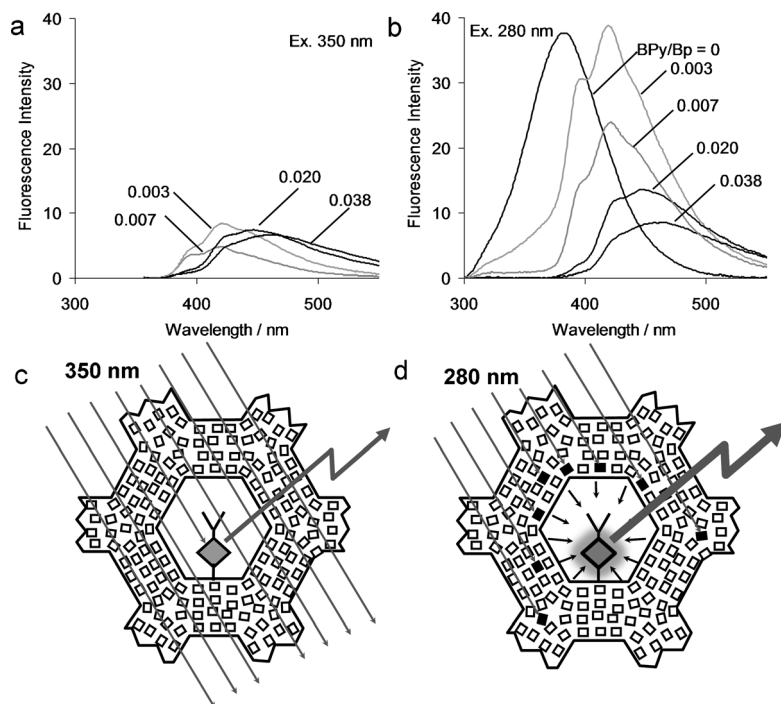


Figure 6. Fluorescence spectra of BPy/Bp-PMO powder dispersed in CH_2Cl_2 excited at a) 350 and b) 280 nm, and schematic illustrations of the emission mechanism from BPy/Bp-PMO when excited at c) 350 nm and d) 280 nm.

(Figures 6a and 6c). On the other hand, the 280 nm light was effectively absorbed by Bp-PMO because of the high density of Bp groups and its high absorbance at this wavelength (Figure 2). The excitation energy on a large number of Bp groups was transferred to a few BPy receptors through FRET, which promoted a strong fluorescence emission from the receptor due to the light-harvesting effect (Figures 6b and 6d). The efficient energy transfer from the

Bp groups to the BPy receptors was confirmed by the strong quenching of the fluorescence emission from the Bp groups ($\lambda_{\text{em}}=385$ nm) in BPy/Bp-PMOs (Figure 6b). The energy-transfer efficiencies were estimated to be 68%, 83%, and 99% at BPy/Bp=0.003, 0.007, and 0.020–0.038, respectively, from the quenching rates of the Bp groups emissions (Table S2 in the Supporting Information).

The fluorescence intensity from BPy/Bp-PMO decreased with increasing BPy/Bp ratio (Figure 6b). The decrease in fluorescence intensity was attributed to self-quenching of the BPy receptors in the meso-channels because of the intermolecular interaction at high concentrations, which was confirmed by a large decrease in the fluorescence quantum yield of BPy in Bp-PMOs ($\Phi_{350}=0.73 \rightarrow 0.20$, Table S2 in the Supporting Information) and the red shift of the fluorescence band. Thus, the increase in the loading amount of BPy receptor has a limitation for the enhancement of the fluorescence intensity in the BPy/Bp-PMO system. The light-harvesting property of PMO has a great merit for the enhancement of the fluorescence intensity of the receptor without increasing its loading amount.

Metal-ion detection: Figure 7 shows the changes in the fluorescence spectra of BPy/Bp-PMO powder (0.003) dispersed in CH_2Cl_2 upon titration of a $\text{Cu}(\text{OAc})_2$ solution. The enhanced fluorescence was largely quenched at very low concentrations

of Cu^{2+} ions ($0\text{--}1.2 \times 10^{-6}$ M) when excited at 280 nm (Figure 7a), whereas the changes in the fluorescence intensity were very small when excited at 350 nm (Figure 7b). This clearly indicates the enhanced detection of Cu^{2+} ions through the light-harvesting effect of PMO. The weak fluorescence at 385 nm observed after quenching was the unquenched emission from the Bp groups in Bp-PMO arising from the low receptor concentrations (Figure 7a).

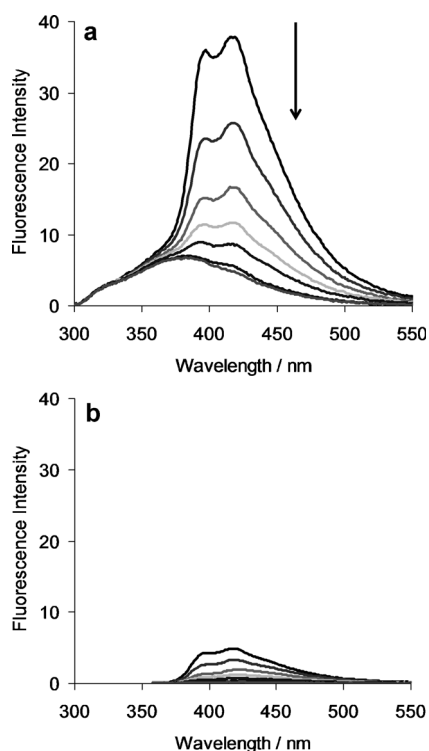


Figure 7. Changes in fluorescence spectra of BPy/Bp-PMO (BPy/Bp = 0.003) powder dispersed in CH_2Cl_2 upon titration of $\text{Cu}(\text{OAc})_2$. The concentrations of $\text{Cu}(\text{OAc})_2$ in the dispersions were 0, 0.15, 0.3, 0.45, 0.6, 0.9, and 1.2×10^{-6} M. The excitation wavelengths were a) 280 nm and b) 350 nm.

Figure 8a shows the change in the enhanced fluorescence spectrum of BPy/Bp-PMO dispersed in CH_2Cl_2 upon titration of a $\text{Zn}(\text{OAc})_2$ solution. The addition of Zn^{2+} caused a gradual decrease in the fluorescence band at around 420 nm, with the concomitant formation of a new fluores-

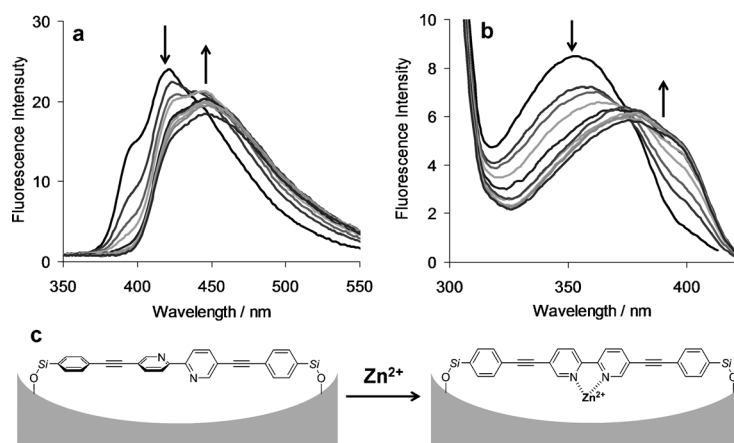


Figure 8. Changes in fluorescence a) emission (excitation wavelength of 280 nm) and b) excitation (detected emission wavelength of 420 nm) spectra of BPy/Bp-PMO (BPy/Bp = 0.007) powder dispersed in CH_2Cl_2 upon titration with $\text{Zn}(\text{OAc})_2$. The concentrations of $\text{Zn}(\text{OAc})_2$ in the dispersions were 0, 0.3, 0.6, 0.9, 1.5, 2.1, 3.0, 3.9, 4.8, and 6.0×10^{-6} M. The detected emission and excitation wavelengths were 431 and 280 nm, respectively. c) Planarization of BPy ligand upon binding with Zn^{2+} .

cence band at around 470 nm. The excitation spectrum (Figure 8b) also showed a decrease in the absorption band at around 350 nm, with the concomitant formation of a new red-shifted absorption band at around 400 nm through an isosbestic point at 375 nm. A similar systematic change in the spectra was observed for homogeneous solution systems with dissolved BPy-containing molecules^[24] and polymers^[25] upon the addition of Zn^{2+} . The spectral red shift is understood as an enhanced planarity of the BPy unit and the resulting change in the electron density upon 1:1 metal complexation, as shown in Figure 8c. The Job's plot of BPy/Bp-PMO with Zn^{2+} was obtained from the fluorescence intensities at 400 nm (new band) in excitation spectra measured under a constant combined BPy and Zn^{2+} concentration ($[\text{BPy}] + [\text{Zn}^{2+}]$) of 3.0×10^{-6} M (Figure S2 in the Supporting Information). The plot shows a typical curve with a maximum at the molar ratio of 0.5, which indicates typical 1:1 complexation between the BPy ligand and Zn^{2+} . The iterative least-squares curve-fitting method (Figure S3 in the Supporting Information) gave an association constant of $2.8 \times 10^6 \text{ M}^{-1}$ for BPy/Bp-PMO and Zn^{2+} , which is higher than the reference value ($2.2 \times 10^5 \text{ M}^{-1}$) of an unmodified BPy solution for Zn^{2+} .^[24b] To the best of our knowledge, this is the first example of a systematic spectral change of BPy ligands attached onto the surface of a solid material upon the titration of metal ions. The systematic spectral change through 1:1 complexation in BPy/Bp-PMO suggests a very weak interaction between the BPy ligands and the surface silanol groups of Bp-PMO, in contrast to BPy adsorbed on silica, which was reported to interact with the surface silanol groups to form ternary surface complexes involving BPy, silanol groups, and metal ions.^[30] This was probably a result of the well-defined pore surface structure and the low concentration of silanol groups in the PMO. The systematic spectral change with minimal influence from the surface silanol groups of BPy/Bp-PMO is advantageous for applications in chemosensors.

Figure 9 shows the fluorescence spectra of BPy/Bp-PMOs upon the addition of various metal ions. Red shifts similar to that observed for Zn^{2+} were observed for Ag^+ , Hg^{2+} , Cd^{2+} , and Pd^{2+} , but strong fluorescence quenching occurred only for Cu^{2+} . Complexes of Zn^{2+} , Hg^{2+} , Cd^{2+} , and Ag^+ with a closed-shell d^{10} configuration are often emissive, whereas that of Cu^{2+} with a partially filled d^9 shell often is not.^[24,25] Eu^{3+} gave almost no change in the fluorescence spectrum because of its weak binding to the 2,2'-bipyridyl unit in the presence of methanol.^[31] The dependence of the spectral change of the fluorescence on the metal ions was similar to that observed for the BPy-derivative molecule^[24] and BPy-modified polymer^[25] reported by Smith's group. They reported a 44 nm red shift of the emission upon the addition of divalent d^{10} metal ions of Zn^{2+} , Hg^{2+} , and Cd^{2+} , accompanied by an increase in the emission intensity when the new absorption band was excited at 420 nm. This suggests that the BPy ligand in Bp-PMO has similar binding properties with metal ions to those of molecules and polymers.

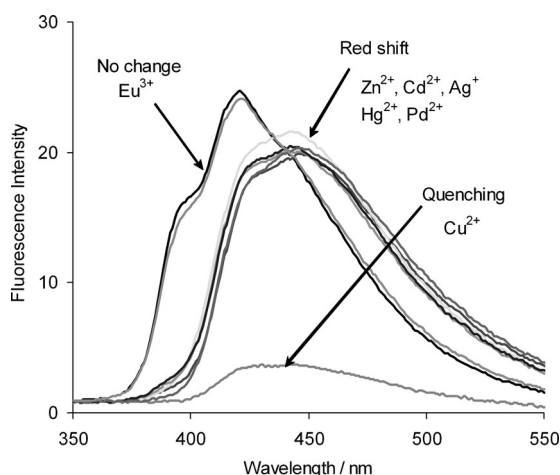


Figure 9. Fluorescence spectra of BPy/Bp-PMO powder (0.007) dispersed in CH_2Cl_2 upon the addition of $\text{Eu}(\text{OTf})_3$, $\text{Zn}(\text{OAc})_2$, $\text{Cd}(\text{OAc})_2$, AgOTf , $\text{Hg}(\text{OAc})_2$, $\text{Pd}(\text{OAc})_2$, or $\text{Cu}(\text{OAc})_2$ ($3.0 \times 10^{-6} \text{ M}$). The excitation wavelength was 280 nm.

Conclusion

We have reported the enhanced fluorescence detection of metal ions using a light-harvesting PMO. A newly designed fluorescent receptor containing a BPy ligand was attached onto the pore walls of Bp-PMO. The emission of the fluorescent BPy receptor in Bp-PMO was successfully enhanced by the light-harvesting effect. The enhanced emission of the BPy receptor was quenched upon the addition of a low concentration of Cu^{2+} . Systematic changes in the enhanced fluorescence emission and excitation spectra were also observed upon the addition of Zn^{2+} and other metal ions. PMOs have a merit in terms of the flexibility of sensor design by appropriate selection of the fluorescent receptor in the mesochannels and the framework organic group of PMOs. It will be very interesting to explore the special features of light-harvesting PMOs for applications as supporting materials for dedicated fluorescence chemosensors.

Experimental Section

General: All reagents and solvents were commercially available and used without further purification. ^1H and ^{13}C NMR spectra were measured using a JEOL ECX-400 spectrometer, operated at 400 and 100 MHz, respectively. Solid-state NMR analyses were performed by ^{29}Si MAS and ^{13}C CP MAS NMR spectroscopy (Bruker ADVANCE 400). Nitrogen adsorption and desorption isotherms were measured on a Quantachrome Nova 3000e sorptometer at -196°C . Prior to the measurements, all the samples were outgassed at 60°C for 6 h. XRD patterns were recorded on a Rigaku RINT-TTR diffractometer using $\text{Cu}_{\text{K}\alpha}$ radiation (50 kV, 300 mV). UV/Vis absorption and fluorescence spectra were measured using JASCO V-670 and JASCO FP-6500 spectrometers, respectively.

Synthesis of 5,5'-bis[4-(diallylethoxysilyl)phenylethynyl]-2,2'-bipyridine (1): Benzene (63 mL) and $i\text{Pr}_2\text{NH}$ (21 mL) were added to a mixture of 5,5'-dibromo-2,2'-bipyridine (0.45 g, 1.44 mmol), $\text{Pd}(\text{PPh}_3)_4$ (0.33 g, 0.29 mmol), and 1-diallylethoxysilyl-4-ethynylbenzene^[26] (0.81 g, 3.17 mmol) under a nitrogen atmosphere. The reaction mixture was

heated under reflux for 40 h. After being cooled to room temperature, the reaction mixture was quenched with water. The organic layer was diluted with CH_2Cl_2 , and the solution was washed with water, dried over anhydrous MgSO_4 , and concentrated under reduced pressure. The residue was chromatographed on silica gel (hexane/ CH_2Cl_2 =1:2) to give 5,5'-bis[4-(diallylethoxysilyl)phenylethynyl]-2,2'-bipyridine (**1**) (802 mg, 84%) as a yellow solid. IR (neat): $\tilde{\nu}_{\text{max}}$ =3076, 2972, 2920, 2877, 2216, 1630, 1585, 1529, 1495, 1462, 1417, 1390, 1363, 1153, 1101, 1078, 1020, 991, 949, 930, 895, 843, 822, 764 cm^{-1} ; ^1H NMR (400 MHz, CDCl_3): δ =8.82 (d, J =1.8 Hz, 2H), 8.44 (d, J =8.2 Hz, 2H), 7.95 (dd, J =8.2 Hz, 1.8 Hz, 2H), 7.61–7.56 (m, 8H), 5.87–5.76 (m, 4H), 4.99–4.91 (m, 8H), 3.79 (q, J =7.1 Hz, 4H), 1.95 (d, J =8.2 Hz, 8H), 1.23 ppm (t, J =7.1, 6H); ^{13}C NMR (100 MHz, CDCl_3): δ =18.4, 21.1, 59.4, 87.3, 93.7, 115.0, 120.4, 120.6, 123.8, 130.8, 132.8, 134.0, 136.4, 139.4, 151.8, 154.1 ppm; HRMS (FAB): m/z calcd for $\text{C}_{42}\text{H}_{45}\text{O}_2\text{N}_2\text{Si}_2$ [$M+H$] $^+$: 665.3014; found: 665.3027.

Preparation of BPy/Bp-PMOs: Bp-PMO was synthesized according to the previous report.^[7a] **1** (3, 6, 30, or 60 mg, 0.0045, 0.009, 0.045, or 0.090 mmol) and trifluoroacetic acid (0.14, 0.28, 1.4, or 2.8 mg) were added to a Bp-PMO (0.14 g) suspension in toluene (12 mL). The suspension was heated under reflux for 24 h and filtered. The resulting solid was washed with AcOEt to remove the unreacted **1**, and dried under vacuum at room temperature for 24 h. The amounts of the binding BPy receptor were measured as follows. The nitrogen contents of BPy/Bp-PMO and Bp-PMO were measured by a Total Nitrogen Analyzer (Mitsubishi, ND-100). The nitrogen content (98 ppm) of Bp-PMO, which was attributed to the residual template surfactant (octadecyltrimethylammonium), was subtracted from the total nitrogen content of BPy/Bp-PMO. The resultant nitrogen content was assumed to originate from BPy.

Metal-ion detection: BPy/Bp-PMO (BPy/Bp=0.003 or 0.007) (4.5 mg) was dispersed in CH_2Cl_2 (100 mL). A MeOH solution of metal salt (e.g., $\text{Cu}(\text{OAc})_2$ or $\text{Zn}(\text{OAc})_2$) was added to the suspension, and the changes in its fluorescence spectra were monitored.

- [1] B. J. Scott, G. Wirnsberger, G. D. Stucky, *Chem. Mater.* **2001**, *13*, 3140–3150.
- [2] L. Basabe-Desmonts, D. N. Reinhoudt, M. Crego-Calama, *Chem. Soc. Rev.* **2007**, *36*, 993–1017.
- [3] W. S. Han, H. Y. Lee, S. H. Jung, S. J. Lee, J. H. Jung, *Chem. Soc. Rev.* **2009**, *38*, 1904–1915.
- [4] a) S. Inagaki, S. Guan, Y. Fukushima, T. Ohsuna, O. Terasaki, *J. Am. Chem. Soc.* **1999**, *121*, 9611–9614; b) T. Asefa, M. J. MacLachlan, N. Coombs, G. A. Ozin, *Nature* **1999**, *402*, 867–871; c) B. J. Melde, B. T. Holland, C. F. Blanford, A. Stein, *Chem. Mater.* **1999**, *11*, 3302–3308; d) S. Inagaki, S. Guan, T. Ohsuna, O. Terasaki, *Nature* **2002**, *416*, 304–307.
- [5] a) F. Hoffmann, M. Cornelius, J. Morell, M. Fröba, *Angew. Chem.* **2006**, *118*, 3290–3328; *Angew. Chem. Int. Ed.* **2006**, *45*, 3216–3251; b) S. Fujita, S. Inagaki, *Chem. Mater.* **2008**, *20*, 891–908.
- [6] T. Tani, N. Mizoshita, S. Inagaki, *J. Mater. Chem.* **2009**, *19*, 4451–4456.
- [7] a) M. P. Kapoor, Q. Yang, S. Inagaki, *J. Am. Chem. Soc.* **2002**, *124*, 15176–15177; b) Y. Goto, N. Mizoshita, O. Ohtani, T. Okada, T. Shimada, T. Tani, S. Inagaki, *Chem. Mater.* **2008**, *20*, 4495–4498; c) N. Mizoshita, Y. Goto, M. P. Kapoor, T. Shimada, T. Tani, S. Inagaki, *Chem. Eur. J.* **2009**, *15*, 219–226.
- [8] N. Mizoshita, Y. Goto, T. Tani, S. Inagaki, *Adv. Funct. Mater.* **2008**, *18*, 3699–3705.
- [9] N. Mizoshita, Y. Goto, Y. Maegawa, T. Tani, S. Inagaki, *Chem. Mater.* **2010**, *22*, 2548–2554.
- [10] D. Chandra, T. Yokoi, T. Tatsumi, A. Bhaumik, *Chem. Mater.* **2007**, *19*, 5347–5354.
- [11] D. Brühwiler, G. Calzaferri, T. Torres, J. H. Ramm, N. Gartmann, L.-Q. Dieu, I. López-Duarte, M. V. Martínez-Díaz, *J. Mater. Chem.* **2009**, *19*, 8040–8067.
- [12] P. N. Minoofar, R. Hernandez, S. Chia, B. Dunn, J. I. Zink, A.-C. Franville, *J. Am. Chem. Soc.* **2002**, *124*, 14388–14396.

- [13] S. Inagaki, O. Ohtani, Y. Goto, K. Okamoto, M. Ikai, K. Yamanaka, T. Tani, T. Okada, *Angew. Chem.* **2009**, *121*, 4102–4106; *Angew. Chem. Int. Ed.* **2009**, *48*, 4042–4046.
- [14] a) H. Takeda, Y. Goto, Y. Maegawa, T. Ohsuna, T. Tani, K. Matsumoto, T. Shimada, S. Inagaki, *Chem. Commun.* **2009**, 6032–6034; b) Y. Maegawa, N. Mizoshita, T. Tani, S. Inagaki, *J. Mater. Chem.* **2010**, *20*, 4399–4403.
- [15] H. Takeda, M. Ohashi, T. Tani, O. Ishitani, S. Inagaki, *Inorg. Chem.* **2010**, *49*, 4554–4559.
- [16] N. Mizoshita, Y. Goto, T. Tani, S. Inagaki, *Adv. Mater.* **2009**, *21*, 4798–4801.
- [17] E. Brasola, F. Mancin, E. Rampazzo, P. Tecilla, U. Tonellato, *Chem. Commun.* **2003**, 3026–3027.
- [18] R. Méallet-Renault, R. Pansu, S. Amigoni-Gerbier, C. Larpent, *Chem. Commun.* **2004**, 2344–2345.
- [19] P. Grandini, F. Mancin, P. Tecilla, P. Scrimin, U. Tonellato, *Angew. Chem.* **1999**, *111*, 3247–3250; *Angew. Chem. Int. Ed.* **1999**, *38*, 3061–3064.
- [20] M. Crego-Calama, D. N. Reinhoudt, *Adv. Mater.* **2001**, *13*, 1171–1174.
- [21] Y. Zheng, J. Orbulescu, X. Ji, F. M. Andreopoulos, S. M. Pham, R. M. Leblanc, *J. Am. Chem. Soc.* **2003**, *125*, 2680–2686.
- [22] G. D. D'Ambruoso, D. V. McGrath, *Adv. Polym. Sci.* **2008**, *214*, 87–147.
- [23] S. W. Thomas III, G. D. Joly, T. M. Swager, *Chem. Rev.* **2007**, *107*, 1339–1386.
- [24] a) A. Ajayaghosh, P. Carol, S. Sreejith, *J. Am. Chem. Soc.* **2005**, *127*, 14962–14963; b) A. E. Dennis, R. C. Smith, *Chem. Commun.* **2007**, 4641–4643; c) S. Sreejith, K. P. Divya, A. Ajayaghosh, *Chem. Commun.* **2008**, 2903–2905.
- [25] S. He, S. T. Iacono, S. M. Budy, A. E. Dennis, D. W. Smith Jr., R. C. Smith, *J. Mater. Chem.* **2008**, *18*, 1970–1976.
- [26] N. Tanaka, N. Mizoshita, Y. Maegawa, T. Tani, S. Inagaki, Y. R. Jorapur, T. Shimada, *Chem. Commun.* **2011**, *47*, 5025–5027.
- [27] Y. Maegawa, T. Nagano, T. Yabuno, H. Nakagawa, T. Shimada, *Tetrahedron* **2007**, *63*, 11467–11474.
- [28] T. Shimada, K. Aoki, Y. Shinoda, T. Nakamura, N. Tokunaga, S. Inagaki, T. Hayashi, *J. Am. Chem. Soc.* **2003**, *125*, 4688–4689.
- [29] B. Onida, L. Borello, C. Busco, P. Ugliengo, Y. Goto, S. Inagaki, E. Garrone, *J. Phys. Chem. B* **2005**, *109*, 11961–11966.
- [30] N. N. Vlasova, *J. Colloid Interface Sci.* **2001**, *233*, 227–233.
- [31] B. Wang, M. R. Wasielewski, *J. Am. Chem. Soc.* **1997**, *119*, 12–21.

Received: August 11, 2011

Revised: October 4, 2011

Published online: January 13, 2012